Toxicology Reports 3 (2016) 63–77

Contents lists available at ScienceDirect

Toxicology Reports

journal homepage: www.elsevier.com/locate/toxrep

Hepatoprotective effect of grape seed proanthocyanidins on Cadmium-induced hepatic injury in rats: Possible involvement of mitochondrial dysfunction, inflammation and apoptosis

Selvaraj Miltonprabu *, Nazimabashir, Vaihundam Manoharan

Department of Zoology, Faculty of Science Annamalai University, Annamalainagar, 608002 Tamilnadu, India

ARTICLE INFO

Article history:
Received 31 August 2015
Received in revised form
24 November 2015
Accepted 28 November 2015
Available online 2 December 2015

Keywords:
Cd
GSP
Mitochondria
Oxidative stress
Liver
Rats

ABSTRACT

The present study was undertaken to evaluate the possible ameliorative role of grape seed proanthocyanidins (GSP) against Cadmium (Cd) induced hepatic inflammation, apoptosis and hepatic mitochondrial toxicity in rats. Male Wistar rats were distributed in four experimental groups: control, GSP, Cd and Cd + GSP. Exposure to a hepatotoxic dose of Cd (5 mg/kg BW) caused liver damage, coupled with enhanced reactive oxygen species (ROS) generation, increased inflammation and apoptosis in liver with increased DNA damage in hepatocytes of rats. Mitochondria were isolated from the hepatic tissues of rats from each group. Our results showed significant decrease in the tri-carboxylic acid cycle enzymes, increased mitochondrial swelling, inhibition of cytochrome c oxidase activity and complex I–III, II–III and IV mediated electron transfer, decreased mitochondrial ATPases, a reduction in calcium content and mitochondrial oxygen consumption in Cd treated rats. All these molecular changes caused by Cd were alleviated by the pre-supplementation with GSP (100 mg/kg BW). The ultra structural changes in the liver also support our findings. From our results, it is clearly indicated that the free radical scavenging, metal chelating and antioxidant potentials of GSP might be the possible reason, responsible for the rescue action against Cd induced mitochondrial damage in the liver of rats.

1. Introduction

Cadmium (Cd) is one of the most toxic metals released into the environment and is known to be a hepatotoxic facet that can be transferred between various levels of the food chain. Cd belongs to the group of transition elements and adopts almost only one oxidation state +2 [1]. The toxic action of the Cd is recognized to be multifactorial. Cd acts as a catalyst in the oxidative reactions of biological micro molecules and therefore toxicities associated with this metal might be due to the oxidative tissue damage. Cd increases the production of reactive oxygen species (ROS) not through the Fenton like reaction [1], but the mechanism involves the interference with the activities of antioxidant, pro-oxidant and some other enzymes, alteration in thiol proteins, inhibition of energy metabolism and alteration in DNA structure and inhibits the activity of several crucial enzymes of the antioxidative defense system. Binding of Cd to sulphydryl group results in the primary injury of cells in mitochondria and secondary injury initiated by the activation of Kupffer cells have been mentioned as a possible mechanism of Cd induced toxic effects [2]. Activated Kupffer cells release proinflammatory cytokines and chemokines, which stimulate the migration and accumulation of neutrophils and monocytes in the liver, which amplificate the Cd, induced primary injury in hepatocytes [3]. The liver is one of the major target organs of both chronic and acute Cd exposure. While hepatocytes and endothelial cells of the liver sinusoids are supposed to be the primary cellular targets in liver [4].

Mitochondria are the key intracellular targets for different stresses, including Cd [5], but the mechanism of metal-induced mitochondrial damage is not fully understood. Mitochondria are the major source of ROS and thus a prime target of Cd induced hepatoxicity. About 1–4% of total consumed mitochondrial oxygen is incompletely reduced to the production of ROS [5]. Cd causes mitochondrial swelling, decreases the expression of genes that control mitochondrial activity, and finally, decreases mitochondrial oxidative capacity and ATP synthesis. Cd insult to mitochondria pertains to a structural damage as well as impairment in the activity of certain enzymes [6] modifies mitochondrial function and inhibits oxidative phosphorylation in the liver of rats.

* Corresponding author. Fax: +91 4144 238080
E-mail addresses: smprabu73@gmail.com, miltonprabu@hotmail.com (S. Miltonprabu).

http://dx.doi.org/10.1016/j.toxrep.2015.11.010

As oxidative stress is one of the key mechanisms of Cd-induced damages, it can be expected that the administration of some antioxidants should be an imperative therapeutic approach. Proanthocyanidins also called condensed tannins and are the oligomers of flavan-3-ol units. They are naturally occurring plant metabolites widely available in fruits, vegetables, nuts and barks and seeds. Grape seed constitutes the major proportion of proanthocyanidins. They are a class of phenolic compounds that takes the form of oligomers or polymers of polyhydroxy flavan-3-ol units, such as (+)-catechin and (−)-epicatechin, all of which contain water soluble molecules and a number of phenolic hydroxyls [7]. Current studies have shown that grape seed proanthocyanidin (GSP) can clear off free radicals, protect the over-oxidative damage caused by free radicals and prevent a range of diseases such as myocardial infarction, atherosclerosis, drug-induced liver and kidney injury [8]. In vivo studies have shown that GSP is a better free radical scavenger and inhibitor of oxidative tissue damage than vitamin C, vitamin E succinate, vitamin C and vitamin E succinate combined, and beta carotene [9]. One of the most advantageous features of proanthocyanidin free radical scavenging activity is that it is easily incorporated within the cell membranes [9]. The presence of both, hydrophobic and hydrophilic residues within the flavan-3-ol molecule, allows these compounds to interact with phospholipid head groups and be adsorbed onto the surface of membranes [10]. Several authors have studied the mitoprotective effect of some types of flavonoids, such as resveratrol [11] and quercetin [12]. These studies suggest that these natural compounds increase the aerobic capacity of muscle tissue and improve the mitochondrial function. Despite the prior research findings, very little is known about the protective effect of GSP against Cd induced mitochondrial oxidative stress in rats.

Previously, we have evaluated the parameters of oxidative stress in the course of Cd-induced hepatotoxicity, as well as the effect of GSP treatment on liver function, lipid peroxidation and activities of antioxidants in the liver of Cd intoxicated rats [10]. The results of our previous study serve as a step toward the development of a mechanism-based therapeutic approach against Cd induced mitochondrial toxicity in the liver of rats. Hence, provide the basis for the usefulness of GSP antioxidant therapy against Cd intoxication. The current study focused on the potential role of GSP against oxidative stress mediated mitochondrial toxicity and the therapeutic approach against Cd induced hepatic apoptosis, inflammation and DNA damage in the liver of rats.

2. Material and methods

2.1. Chemicals

GSP, containing approximately 54% dimeric, 13% trimeric procyanidins, and 7% tetrameric, proanthocyanidins were obtained from Jianfeng, Inc. (Lot No. G050412, Tianjin, China). $CdCl_2$ and other fine chemicals were obtained from Pfizer, India. Cytochrome c oxidase and Sigma diagnostics (I) Pvt., Ltd., Baroda, India, and Caspase-3 assay, all were obtained from the Sigma Aldrich Chemical Co. (St. Louis, MO). Reduced nicotinamide adenine dinucleotide (NADH) and sucrose were purchased from Himedia Laboratories Pvt., Ltd. (Mumbai, India). All other analytical grade chemicals were purchased from E. Merck (India).

2.2. Animals

Male Wistar rats weighing 170–190 g were used in this study for 28 days. They were maintained in an environmentally controlled animal house (temperature 24°–38 °C, Humidity 55 ± 10%) with a 12 h light/dark schedule and free access to deionized drinking water. The animal treatment and protocol employed were approved by the institutional Animal Ethics Committee, Annamalai university (Registration number: 1020/2013, CPCSEA).

2.3. Experimental design

In the present study, Cd was administered as $CdCl_2$ and administered intragastrically at a dose of 5 mg/kg body weight (BW)/day for 28 days. Twenty four male Wistar rats were divided into four groups consisting of six rats in each group:

Group I—served as a control group and received normal saline used as a vehicle, once in a day, for four weeks continuously.

Group II—rats were orally administered with GSP (100 mg/kg BW) in normal saline once a day for four consecutive weeks [10]

Group III—were orally administered with Cd as $CdCl_2$ (5 mg/kg BW) dissolved in saline once a day for four weeks [13]

Group IV—were orally pre-administrated with GSP (100 mg/kg BW) 90 min before the Cd (5 mg/kg.BW) once in a day for four weeks.

The animals from all the groups were provided with a pellet foodstuff from the Amrut laboratory animal feed, Pune, Maharashtra, India for feeding and water *ad libitum*. At the end of the experimental period, rats were fasted overnight and were anesthetized with pentobarbital sodium (35 mg/kg, IP) and euthanized by cervical decapitation. Blood was collected in tubes containing ethylene diamine tetraacetate (EDTA). The plasma was obtained after centrifugation (2000 × *g* for 20 min at 4 °C) and liver tissues were excised immediately and rinsed in ice-chilled physiological saline.

2.4. Cd concentration in the liver

Samples of the liver (about 100 mg) were weighed in Teflon PFA microwave digestion vessels previously washed in an ultrasonic bath for 30 min, rinsed in MilliQ water, left overnight in 10% ultrapure HNO_3, rinsed again with MilliQ water and left to dry at room temperature in a laminar flow hood. Samples were digested using 10 ml of HNO_3. The use of HNO_3 for digestion of biological samples is widely favored as it introduces less interference than other mineral acids in the analysis of biological samples by inductively coupled plasma mass spectrometry (ICP-MS) [14]. After cooling, the vessels were opened in a laminar flow box. The contents were transferred to acid cleaned polypropylene tubes and diluted to a volume of 10 ml with MilliQ water. All samples were diluted (1:4). For ICPMS, standards were prepared manually. Cd concentration was determined by the ICPMS method (ELAN-6000 model, PerkinElmer, Sciex, Toronto, Canada) according to the manufacturer's recommendation. The detection limit was 0.08 lg Cd/L. Daily controls ensured that the instrument satisfied the manufacturer's recommendations on performance criteria

2.5. Hepatic membrane-bound ATPases estimation

The sediment after centrifugation was resuspended in ice-cold Tris (hydroxymethyl) aminomethane (Tris)–hydrochloric acid (HCl) buffer (0.1 M) pH 7.4. This was used for the estimations of membrane-bound enzymes and protein content. The membrane-bound enzymes such as sodium ion (Na^+)/potassium ion (K^+)-ATPase, calcium ion (Ca^{2+})-ATPase and magnesium ion (Mg^{2+})-ATPase activities were assayed by estimating the amount of phosphorous liberated from the incubation mixture containing tissue homogenate, ATP, and the respective chloride salt of the electrolytes [15] [16]. Total protein content was estimated by the method described by Lowry et al. [17].

2.6. Inflammatory cytokines

Liver tissues from each group were subsequently homogenized in cold potassium phosphate buffer (0.05 M, pH 7.4). The homogenates were centrifuged at 5000 rpm for 10 min at 4 °C. The resulting supernatant from hepatic homogenate was used for determination of nitric oxide (NO), tumor necrosis factor-α (TNF-α) and NF-kB. The levels of TNF-α and NF-kB in tissue homogenates were determined by enzyme-linked immunosorbent assay (ELISA) using a rat immunoassay kit (Biosource International, Inc. Camarillo, California, USA) according to the recommendations of the manufacturer using a Microtiter plate reader capable of reading at 450 nm (Sunrise, Austria) [18]. Tissue TGF-β1 levels were measured by quantitative sandwich ELISA using kits supplied from R&D Systems (Europe, Ltd., United Kingdom) [19]. IL-4 content in tissue was determined according to Nolan et al. [20] by solid phase ELISA using a rat IL-4 kit (RayBiotech, Norcross, USA) and a Microtiter plate reader at 450 nm.

2.7. Hydroxyproline

Hydroxyproline (Hyp) content in hepatic tissues was determined spectrophotometrically by Ehrlich reagent. Briefly, 0.1 g tissues was pulverized ground, 500 μl of 6 N HCl were added and incubated overnight at 120 °C. Acid hydrolysis of collagen liberated Hyp. 5 μl of acid hydrolysate were mixed with 5 μl of citrate acetate buffer and 100 μl chloramines T in ELISA plate and incubated for 20 min at room temperature (oxidation). The oxidation product reacts with *p*-dimethylaminobenzaldhyde (Ehrlich reagent) to produce a colored complex that can be measured in an ELISA plate reader at 550 nm. Concentrations of Hyp were calculated from the plotted standard curve using Hyp standard solution (0–200 μg/ml) [21].

2.8. Immunoblotting of signaling proteins

Proteins (50 μg) from each sample were separated by 10% SDS-PAGE and transferred into PVDF membranes. Membranes were then blocked using BSA and incubated separately with primary antibodies of anti caspase-3, anti-PARP and anti-Bcl-*xL* (1:1000 dilution), anti cytochrome c (1:1000 dilution), anti Bad (1:1000 dilution), anti Bax (1:1000 dilution), anti Bcl-2 (1:1000 dilution) at 4 °C for overnight. The membranes were washed in TBST (50 mmol/L Tris–HCl, pH 7.6, 150 mmol/L NaCl, 0.1% Tween 20) for ~30 min and incubated with appropriate HRP conjugated secondary antibody (1:2000 dilution) for 2 h at room temperature and developed by the HRP substrate 3,3′-diaminobenzidine tetrahydrochloride (DAB) system (Bangalore, India).

2.9. Comet assay

Hepatocytes were isolated from control and experimental groups and processed for the alkaline comet assay as described previously [22]. The slides were immersed in lysis buffer for 1 h at 4 °C and equilibrated in alkaline solution for 20 min, followed by electrophoresis at 18 V and 300 mA (Sub-Cell GT system with Power Pac basic power supply; Bio-Rad Laboratories, Inc., Hercules, California, USA). After electrophoresis, the slides were neutralized and stained by ethidium bromide. The images were captured using a fluorescence microscope (Eclipse TS100; Nikon Instruments Inc., Melville, New York, USA). Fifty images per slide were analyzed for tail length and olive tail moment using image analyzer CASP software version 1.2.2.

2.10. Isolation of hepatic mitochondria

The mitochondria were isolated by the method of Cain and Skilleter [23]. Briefly, liver was minced in 20 ml buffer (0.25 M sucrose, 5 mM Tris–HCl and pH 7.4), homogenized, and then centrifuged at 460 × *g* for 10 min at 4 °C. The retained supernatant was centrifuged at 12,500 × *g* for 7 min. The mitochondrial layer was removed, resuspended, and repelleted at 12,500 × *g* for 7 min. The resultant mitochondrial pellet was then washed and resuspended in the same buffer and was preserved at −70 °C until analyses were made. Fresh mitochondria were used for each experiment. The mitochondria isolated were characterized by respiratory ratio [24]. Rotenone titration experiments were also done to substantiate complex I assay. Sub mitochondrial particles (SMP) were prepared from isolated mitochondria by sonicating (at 4 °C) mitochondrial suspension at 60% frequency 3 times for 10 s each, with an interval of 2 min using a probe sonicator (Dr Heilscher Gmbtt Co., Germany).

2.11. Assay of liver mitochondrial enzymes

The activities of isocitrate dehydrogenase (ICD), succinate dehydrogenase (SDH), malate dehydrogenase (MDH), α-ketoglutarate dehydrogenase (α-KGDH) and NADP were estimated according to the standard procedures of King [25], Reed and Mukherjee [26] and Minakami, et al. [27].

2.12. Coenzymes Q

The extent of Coenzymes Q (Q9 and Q10) were isolated and estimated according to the method of Zhang et al. [28]. Briefly, One ml of 30% tissue homogenate (in 0.25 M sucrose) was put in a tube containing 50 μl butylated hydroxyl toluene (1 mg/ml), to which 1 ml, 0.1 mM sodium dodecyl sulfate (SDS) was added, vortexed for 30 s, sonicated for 15 s, chilled in ice–water and vortexed for 15 s. Two ml of ethanol was added and again vortexed for 30 s, sonicated for 15 s, chilled in ice–water and vortexed for 15 s. Then, 2 ml of hexane was added. The tube was vortexed and subsequently centrifuged at 2000 rpm for 3 min. Hexane layer (1.75 ml) was transferred to another tube and evaporated under the gentle nitrogen stream. Dionex Ultimate 3000HPLC system (Dionex, Germany), using a reverse phase C-18 column (250 × 4.6 mm, particle size 5l) and UV detector was employed for estimation of co-enzymes Q. The samples were dissolved in 100 μl of the mobile phase consisting of HPLC grade methanol and ethanol (70:30), filtered through cellulose nylon membrane filter (0.45 lm) (PALL, Life Sciences) and injected to HPLC. The aliquots of the filtrate were elated with an isocratic solvent mixture comprising methanol: ethanol (70:30).

2.13. Cytochrome C oxidase activity

Cytochrome c oxidase activity was assayed with a colorimetric assay kit purchased from Sigma–Aldrich Chemical Co. (St. Louis, MO). Absorbance was measured by UV-Double Beam Spectrophotometer (Shimadzu, 160A) at 550 nm. Cytochrome c oxidase activity was expressed as U/mL.

2.14. Estimation of mitochondrial Ca^{2+} -ATPase and Na^+/K^+ ATPase activity

The activity of mitochondrial Ca^{2+}-ATPase was studied by the method of Rorive and Kleinzellar [29]. Phosphate liberated during Ca^{2+}-ATPase activity was estimated by the method of Lowry and Lopez [30]. Mitochondrial Na^+/K^+-ATPase [15] was also estimated in liver mitochondria isolate.

2.15. Estimation of mitochondrial calcium content

Atomic Absorption Spectrometer (PerkinElmer, Analyst 200) was used to estimate the calcium content of mitochondrial samples by using the method of Zydowo et al. [31] described elsewhere.

2.16. Determination of mitochondrial permeability transition

Mitochondrial swelling as an indicator of mitochondrial permeability transition (MPT) was estimated by measuring the decrease in absorbance at 540 nm. The changes of mitochondrial MPT were measured by following the methods of Petit, et al. [32]. For the detection of mitochondrial swelling, mitochondria were resuspended in the buffer (400 mM mannitol, 10 Mm KH_2PO4, and 5 mg/ml BSA, and 50 mM Tris–HCl, pH 7.2, 4 °C) at a concentration of 100 μg proteins/10 μl for 30 min. For determination of mitochondrial MPT, 1 mg mitochondrial protein was suspended in test buffer [200 mM sucrose, 10 mM Tris-3-(*N*-morpholino) propane sulfonic acid (MOPS), pH 7.4, 5 mM succinate–Tris, 1 mM Tris–Phosphate (Pi), 10 μM ethyleneglycolbis (aminoethylether)-tetraacetic acid (EGTA)-Tris, 2 μM rotenone, 1 μg/mL oligomycin], and the changes of absorbance at 540 nm were monitored before and after the addition of 150 μM $CaCl_2$ using UV-Double Beam Spectrophotometer (Shimadzu 160A).

2.17. Detection of mitochondrial membrane potential (ΔYm)

The mitochondrial membrane potential (ΔΨm) was detected by monitoring the fluorescence quenching of Rh 123 dynamically [33]. Fluorescence with excitation at 503 nm and emission at 527 nm was detected in a reaction buffer (containing 250 mM sucrose, 2 mM HEPES, 0.5 mM KH_2PO_4, 4.2 mM sodium succinate, pH 7.4, and 0.3 μm Rh 123) using F-4500 FL Spectrophotometer (Hitachi High-Technologies Corporation). Then mitochondria was added to 0.5 mg/ml in the buffer and incubated for 3 min. The fluorescence was recorded again, and the alteration of the ΔΨm was detected by the decrease of fluorescence.

2.18. Mitochondrial oxygen consumption

By using a Clark oxygen electrode (YSI Model 53 Oxygen Monitor, USA), mitochondrial respiration was monitored in the media (225 mM sucrose, 20 mM KCl, 5 mM $MgCl_2$, 10 mM KH_2PO_4, 10 mM HEPES (pH 7.4) and 2 μM rotenone) at 25 °C [34].

2.19. Respiratory complexes activity

For the determination of NADH-cytochrome c reductase (complex I–III), 0.02 mg ml^{-1} MM was added to 100 mM KH_2PO_4–K_2HPO_4(pH 7.4), 25 μM cytochrome c^{3+} and 0.5 mM KCN, and observed spectrophotometrically at 550 nm (ε = 19.6 mM^{-1} cm^{-1}) and 30 °C. Enzymatic activity was expressed as nmol reduced cytochrome c^{3+} per min mg protein. Succinate cytochrome c reductase activity (complex II–III) was similarly determined and expressed, except that NADH was substituted by 5 mM succinate. The activity was expressed as nmol reduced cytochrome c^{3+} per min mg protein. Cytochrome oxidase activity (complex IV) was assayed spectrophotometrically at 550 nm by following the oxidation rate of 50 mM cytochrome c^{2+} 21 in 0.1 M K_2HPO_4–KH_2PO_4 (pH 7.4), 50 μM cytochrome c^{2+} and 0.02 mg ml^{-1} MM. Results were expressed as k (min^{-1}) mg^{-1} protein.

2.20. Estimation of mitochondrial ROS generation

One of the widespread methods in detecting ROS production by mitochondria is based on 2′ 7′- dichloroflourescein (H2DCFDA) oxidation [35] H2DCFDA, an uncharged, cell-permeable fluorescent probe readily diffuses into cells and gets hydrolyzed by intracellular esterases to yield H2DCF, which is trapped inside the cell. Then it is oxidized from the nonfluorescent form to a highly fluorescent compound dichlorofluoresce in by hydrogen peroxide (H_2O_2) or other low-molecular-weight peroxides produced in the cells. Thus, the fluorescence intensity is proportional to the amount to the H_2O_2 produced by the cell. For normal mitochondria, the reaction mixture contained a respiration buffer (pH 7.2), and mitochondria (500 μg/ml) incubated with or without Cd for 8 min. To this mixture, 20 μM H2DCFDA, 0.4 mM NADH was added and mixed properly and the fluorescence change (λex = 488 nm and λc = 540 nm) was observed for 8 min using a PerkinElmer fluorimeter. The difference in fluorescence intensity was expressed as a% arbitrary fluorescence unit (AFU).

2.21. Electron microscopic examination

Electron microscopic liver specimens were prefixed in 3% glutaraldehyde solution in 0.1 M phosphate buffer for 1.5 h at 4 °C. Following this, they were washed in 0.15 M phosphate buffer (pH 7.2) and post-fixed in 2% osmium tetroxide solution in 10 mM sodium phosphate buffer and left overnight. Dehydration was performed in acetone, and inclusion was done in the epoxy embedding resin Epon. Semi-thin sections of 1 mm thick were cut using an Ultracut E ultratom (Leica) and were stained with toluidine blue. Ultrathin sections were obtained from selected blocks, mounted on copper grids, stained with uranyl acetate and lead citrate and examined using Carl Zeiss 900 transmission electron microscope.

2.22. Ultra structural morphology of mitochondria

Ultra structural morphology of mitochondria was determined by electron microscopy. Liver specimens from control rats and experimental rat were taken and fixed with 4% glutaraldehyde in 0.1 M sodium cacodylate buffer (pH 7.4) for 4 h at 4 °C. After fixation and an overnight wash in sodium cacodylate buffer, the specimens were post fixed with 1% osmium tetroxide in sodium cacodylate buffer for 1 h at 4 °C, dehydrated in alcohol and embedded in araldite resin. And semi thin sections (1 μm) were removed for optical microscopy. Before examination, ultrathin sections were mounted on copper mesh grids and stained with uranyl acetate and lead citrate with electron microscope. The ultra structural morphology of mitochondria was evaluated in five rats of each group and 10 randomly selected electron micrographs of the hepatic lobule were in each rat (15,000× magnification).

2.23. Statistical analysis

Data were analyzed by one way analysis of variance (ANOVA) followed by Duncan's multiple range test (DMRT) for analysis between groups using a commercially available statistics software package (SPSS® for Windows, V. 17.0, Chicago, USA). Results were presented as mean ± SD. $P < 0.05$ was considered as statistically significant.

3. Results

3.1. Cd concentration in the liver

Table 1 shows the effect of Cd and GSP on body weight, organ weight (liver), food and water intake and Cd concentration in control and experimental rats. In Cd treated rats body weight gain, food and water intake were significant ($p < 0.05$) decreased with significant ($p < 0.05$) increase in organ body weight and Cd concentration in the liver of rats. All these changes induced by Cd intoxication

Table 1
Effect of GSP on body weight, organ weight, food and water intake and Cd concentration in control and experimental rats.

Groups	Body weight (g)		Diet intake (g/100 bw/day)	Water intake (ml/rat day)	Organ weight liver (g)	Cd concentration(μg/g wet tissue)
	Initial	Final				
Control	180 ± 10.2	198 ± 12.3	13.12 ± 0.9[a]	19.98 ± 2.5 [a]	2.9 ± 0.2[a]	ND
GSP	189 ± 10.4	199 ± 12.6	12.02 ± 0.8 [a]	18.12 ± 2.2 [a]	2.98 ± 0.3[a]	ND
Cd	188 ± 11.2	170 ± 11.3	8.25 ± 0.7 [b]	12.29 ± 2.7[b]	3.79 ± 0.2[b]	25.14 ± 1.02[a]
Cd + GSP	184 ± 12.5	194 ± 10.3	10.41 ± 0.8[c]	16.28 ± 1.2[c]	3.02 ± 0.4[ac]	15 ± 1.09[b]

Values are mean SD for 6 rats in each group; a, b, c and d. Values are not sharing a common superscript letter (a–d) differ significantly at $p < 0.05$ (DMRT). ND:not detectable.
Values are mean SD for 6 rats in each group; a–d. Values are not sharing a common superscript letter (a–d) differ significantly at $p < 0.05$ (DMRT). ND:not detectable.

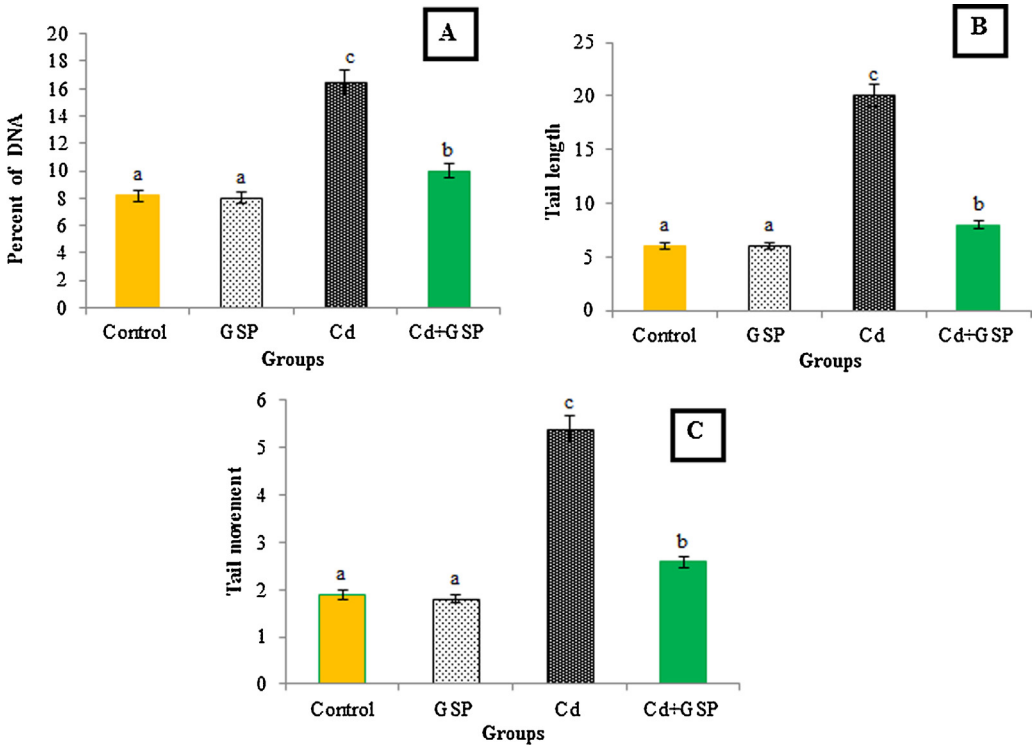

Fig. 1. Effect of GSP and Cd on DNA damage in the hepatocytes of control and experimental rats. (A) % DNA in tail; (B) tail length in micrometers; (C) olive tail moment (arbitrary unit). Values are expressed as mean ± SD for six rats in each group. Values not sharing a common superscript letter (a–d) differ significantly at $p < 0.05$.

were significantly ($p < 0.05$) prevented on preadministration of GSP. GSP alone treated rats and control did not show the accumulation of Cd in the liver.

3.2. Hepatic ATPases in the liver of Cd treated rats

Table 2 shows the levels of total ATPase, Na^+/K^+-ATPase, Mg^{2+}-ATPase, and Ca^{2+}-ATPase in the liver of control and experimental rats. The levels of the membrane-bound ATPases in the liver tissue of Cd-treated rats were significantly decreased ($p < 0.05$) when compared with the control rats. However, pretreatment of GSP in Cd intoxicated rats significantly restored ($p < 0.05$) the levels of all the membrane-bound ATPases when compared with Cd-intoxicated rats. Significant ($p < 0.05$) changes were observed between control and GSP alone treated rats.

3.3. Effect of GSP on hepatic cytokines and hydroxyproline (Hyp) contents

Table 3 shows the levels of hepatic inflammatory markers and Hydroxyproline content in the liver of control and experimental rats. Cd significantly elevated ($p < 0.05$) pro-inflammatory TNF-α, NF-κB, and pro-fibrotic (TGF-β1) cytokines in addition to fibrosis marker (Hyp) and reduced anti-inflammatory (IL-4) contents in hepatic tissues of rats as compared to the control rats. Pretreatment of GSP in Cd intoxicated rat resulted in a significant marked decrement ($p < 0.05$) in hepatic TNF-α, NF-κB as well as TGF- β1 while maintaining balance in Hyp and showed a significant increment ($p < 0.05$) in IL-4 contents, when compared to the Cd alone treated rats.

3.4. DNA damage

Fig. 1 displays the level of DNA damage in control and experimental rats. A significant ($P < 0.05$) increase in different comet assay parameters such as% tail DNA, tail length ((TL) in micrometer), tail moment, and olive tail moment OTM (arbitrary unit) were observed in rats treated with Cd when compared with the control rats. Preadministration of GSP in Cd intoxicated rats significantly ($P < 0.05$) reduced the%DNA in tail, TL, and OTM when compared with Cd alone treated group (Fig. 1). Fig. 2 shows the representative photomicrographs of comets stained with ethidium bromide at 200× magnification showing the DNA migration pattern in hepatocytes, where the control rats show no DNA migration. While extensive DNA migration was observed in Cd-treated rats when compared with the control rats. GSP-preadministration in Cd intoxicated rats shows the minimal DNA migration when compared with Cd alone-treated rats. GSP alone administered rats show no DNA migration.

Table 2
Changes in the levels of hepatic total ATPase, Na+/K+ -ATPase, Mg2+-ATPase and Ca2+-ATPase in the liver of control and experimental rats.

Groups	Normal	GSP	Cd	Cd + GSP
Total ATPases (μg pi liberated/min/mg protein	1.72 ± 0.15^{a}	1.74 ± 0.18^{b}	1.20 ± 0.12^{c}	1.59 ± 0.14^{d}
Na^{+}/K^{+}-ATPase (μg pi liberated/min/mg protein)	0.34 ± 0.05^{a}	0.35 ± 0.09^{b}	0.18 ± 0.02^{c}	0.28 ± 0.04^{d}
Ca^{2+} -ATPase (μg pi liberated/min/mg protein)	0.47 ± 0.06^{a}	0.48 ± 0.07^{b}	0.19 ± 0.01^{c}	0.37 ± 0.07^{d}
Mg^{2+} -ATPase (μg pi liberated/min/mg protein)	0.53 ± 0.02^{a}	0.54 ± 0.03^{b}	0.25 ± 0.05^{c}	0.48 ± 0.07^{d}

Table 3
Changes in the activities of hepatic inflammatory markers and Hydroxyproline content in the liver of control and experimental rats.

Groups	Normal	GSP	Cd	Cd + GSP
No (μmol/mg protein)	0.64 ± 0.05^{a}	0.63 ± 0.04^{b}	0.21 ± 0.18^{c}	0.55 ± 0.08^{d}
IL-4 (pg/mg protein)	45.3 ± 1.29^{a}	46.4 ± 1.09^{b}	18.1 ± 1.25^{c}	39.3 ± 1.15^{d}
TNF-α (pg/mg protein)	8.71 ± 0.2^{a}	7.17 ± 0.41^{b}	39.06 ± 0.81^{c}	16.59 ± 0.42^{d}
TGF-β1 (pg/mg protein)	106 ± 1.67^{a}	107 ± 1.17^{b}	175 ± 1.86^{c}	124.21 ± 1.23^{d}
NF-κB (ng/mg protein)	15.3 ± 0.13^{a}	16.4 ± 0.16^{b}	32.5 ± 0.23^{c}	24.2 ± 0.11^{d}
Hyp (mg/g tissue)	90.16 ± 1.3^{a}	92.6 ± 1.2^{b}	139.2 ± 1.04^{c}	103.1 ± 1.5^{d}

Values are mean ± SD for 6 rats in each group; $^{a-d}$. Values are not sharing a common superscript letter (a–d) differ significantly at $p < 0.05$ (DMRT).

3.5. Liver mitochondrial enzymes

Fig. 3(A and B) shows the levels of mitochondrial citric acid cycle enzymes, isocitrate dehydrogenase (ICD), succinate dehydrogenase (SDH), and malate dehydrogenase (MDH), α- ketoglutarate dehydrogenase (α-KGDH) and respiratory marker enzyme (NADH dehydrogenase) in the mitochondria of control and experimental rats. In Cd intoxicated rats there was a significant ($p < 0.05$) reduction in the activities of TCA cycle enzymes, NADH dehydrogenase and protein when compared with control rats. Interestingly pretreatment of GSP in Cd treated rats significantly ($p < 0.05$) increased the activities of TCA cycle enzymes, NADH dehydrogenase and protein when compared with Cd alone treated rats. GSP alone treated rats showed significant differences ($p < 0.05$) when compared with the control rats.

3.6. Effect on coenzymes Q

The effects of GSP on mitochondrial coenzymes Q (Q9 and Q10) in the liver are shown in Fig. 4, respectively. Total co-enzyme Q9 level was reduced significantly ($p < 0.05$) with increase in the level of Q10 in Cd treated rats as compared to the control rats. Pretreatment of GSP in Cd intoxicated rats significantly ($p < 0.05$) elevated Q9 level and showed decreased ($p < 0.05$) activity of total

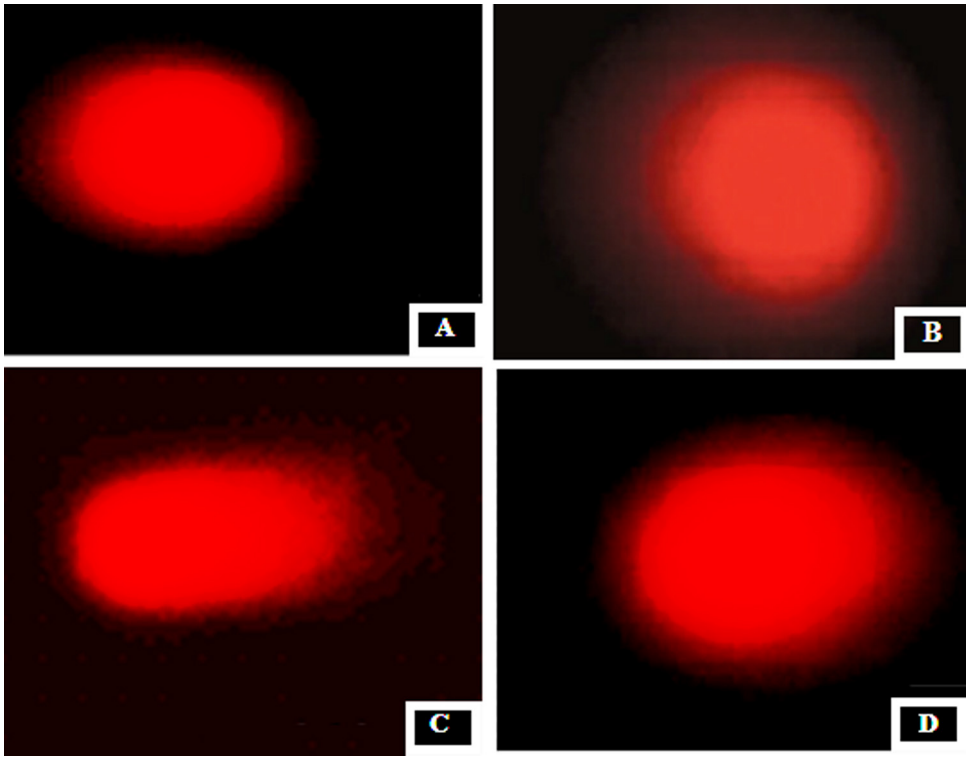

Fig. 2. Representative photomicrographs of comets stained with ethidium bromide at ×200 magnification showing the DNA migration pattern in hepatocytes. (A) Control rats show no DNA migration. (B) GSP alone administered rats show no DNA migration (C) Cd-treated rats show extensive DNA migration. (D) GSP-preadministered Cd intoxicated rats show minimal DNA migration.

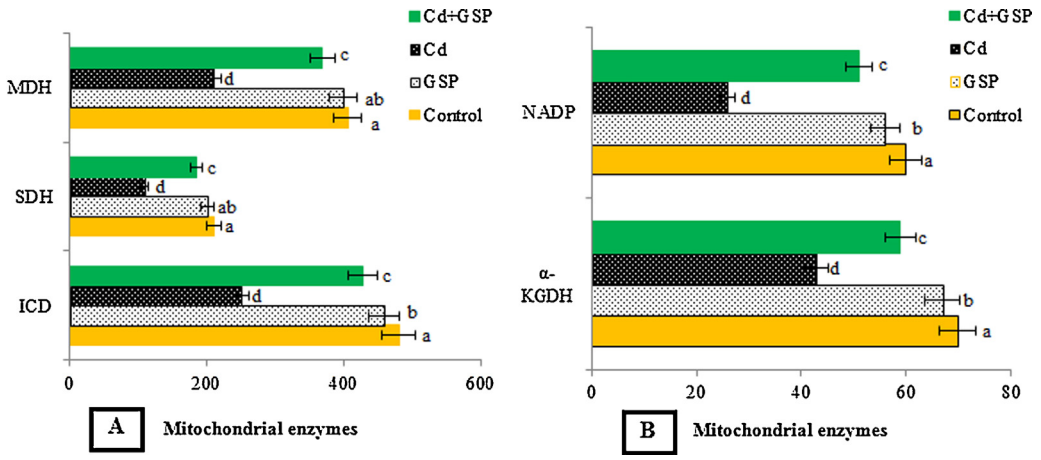

Fig. 3. (A and B). Effects of GSP on Cd induced changes in the activities of mitochondrial enzymes of control and experimental rats. Values are expressed as mean ± SD for six rats in each group. Values not sharing a common superscript letter (a–d) differ significantly at $p < 0.05$ (DMRT). Units for ICD: nM of NADH oxidized/h/mg protein; SDH: nM of succinate oxidized/min/mg protein; MDH: nM of NADH oxidized/min/mg protein; α-KDH: nM of ferro cyanide formed/h/mg protein; NADH dehydrogenase: nM of NADH oxidized/min/mg protein.

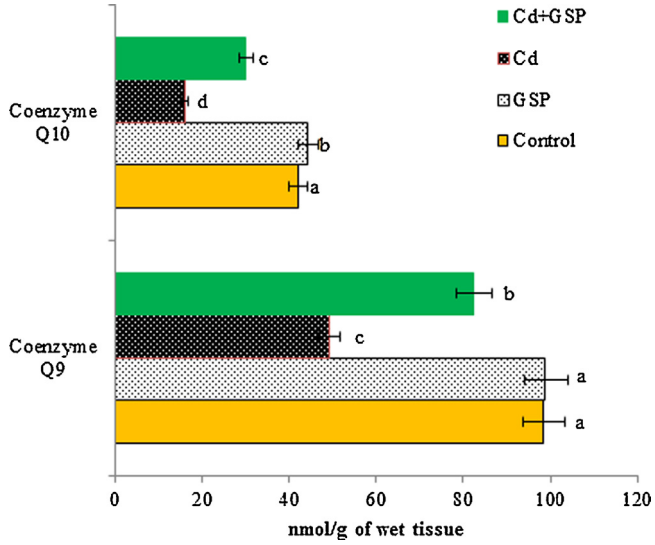

Fig. 4. Effects of GSP on Cd induced changes in the activities of mitochondrial total coenzymes Q10 and Q9 in control and experimental rats. Values are expressed as mean ± SD for six rats in each group. Values not sharing a common superscript letter (a–d) differ significantly at $p < 0.05$ (DMRT).

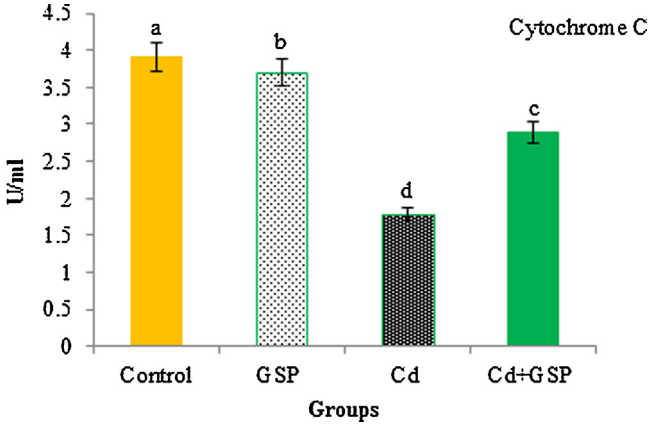

Fig. 5. Effect of GSP on Cd-induced changes in cytochrome c oxidase activity. Values are mean ± S.D. for six rats in each group. Bars not sharing a common superscript letter (a–d) differ significantly at $p < 0.05$ (DMRT).

co-enzyme Q10 in the liver tissue as compared to the control rats. Preadministration of GSP in Cd treated rats significantly ($p < 0.05$) restored the level of co-enzymes in liver tissues as compared to the Cd alone treated rats. GSP alone treated rats showed significant differences ($p < 0.05$) when compared with the control rats.

3.7. Cytochrome C oxidase activity

In Fig. 5, the cytochrome c oxidase activity in Cd intoxicated liver mitochondria of rats was decreased significantly ($p < 0.05$) as compared to the control rats. Preadministration of GSP in Cd intoxicated rats significantly increased the cytochrome c oxidase activity when compared with Cd treated rats. GSP alone treated rats showed significant differences ($p < 0.05$) when compared with the control rats.

3.8. Mitochondrial Ca^{2+}-ATPase and Na^+/K^+ ATPase activity

In Fig. 6, compared with control, Ca^{2+}-ATPase activity and Na^+/K^+ ATPase activity in hepatic mitochondria was inhibited significantly ($p < 0.05$) in Cd-treated rats. Pretreatment of GSP in Cd intoxicated rats significantly ($p < 0.05$) restored the Ca^{2+}-ATPase and Na^+/K^+ ATPase activity (Fig. 4), when compared with Cd alone treated rats. GSP alone treated rats showed significant differences ($p < 0.05$) when compared with the control rats.

3.9. Mitochondrial Ca^{2+} content

In Fig. 7, Mitochondrial calcium content was reduced significantly ($p < 0.05$) in Cd-treated rats, when compared with control rats. The calcium level was significantly ($p < 0.05$) revived as compared to Cd alone treated rats when these Cd-treated rats were pre-supplemented with GSP.

3.10. Mitochondrial permeability transition (MPT)

Fig. 8, shows that compared with control, hepatic mitochondrial swelling rate, an index of MPT, was significantly ($p < 0.05$) increased in Cd-treated group as compared to control rats. Such high swelling rate was significantly ($p < 0.05$) lowered when GSP was preadministered prior to Cd intoxication as compared to the Cd alone treated rats.

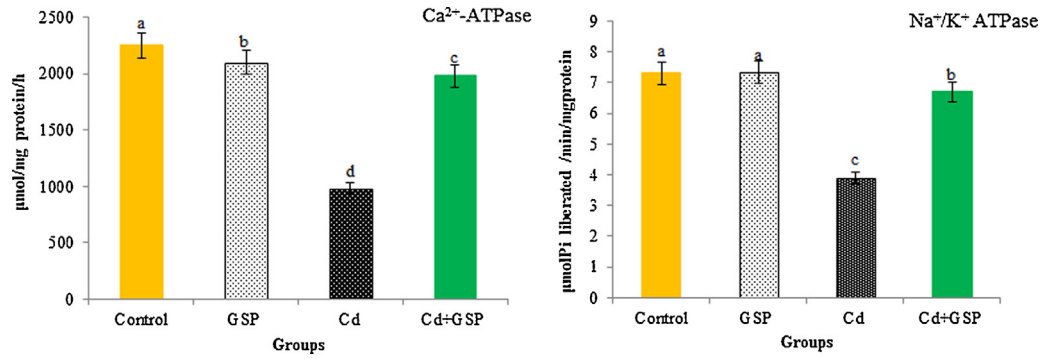

Fig. 6. Effect of GSP on Cd-induced changes in mitochondrial Ca2+-ATPase and Na+/K+- ATPase activity in control and experimental rats. Values are mean ± S.D. for six rats in each group. Bars not sharing a common superscript letter (a–d) differ significantly at $p < 0.05$ (DMRT).

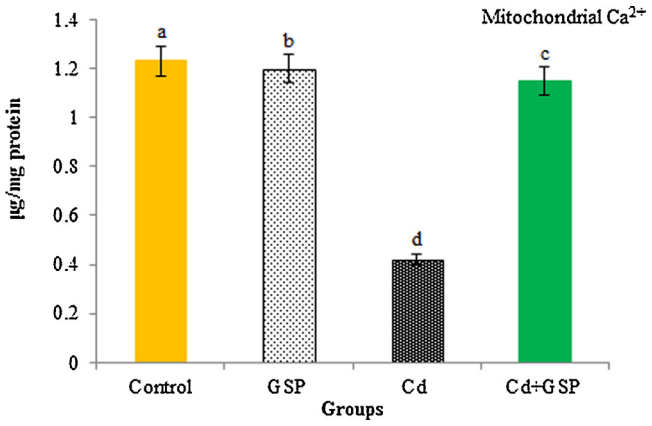

Fig. 7. Effects of GSP on Cd-induced changes in hepatic mitochondrial calcium content. Values are mean ± S.D. for six rats in each group. Bars not sharing a common superscript letter (a–d) differ significantly at $p < 0.05$ (DMRT).

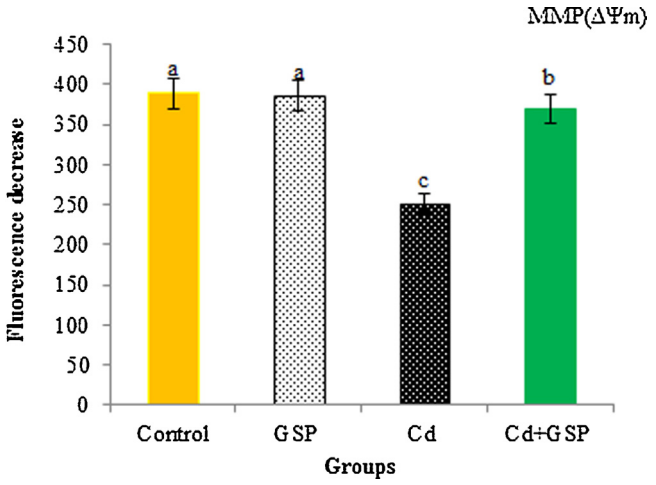

Fig. 9. Effects of GSP treatment on Cd-induced changes in mitochondrial membrane potential (ΔΨm). Values are mean ± S.D. for six rats in each group. Bars not sharing a common superscript letter (a–d) differ significantly at $p < 0.05$ (DMRT).

3.11. Mitochondrial membrane potential (ΔΨm)

In Fig. 9, the initial fluorescence (602 ± 14) dramatically decreased after adding mitochondria, showing alterations in the mitochondrial membrane potential (ΔΨm) of rats. The fluorescence in control group declined about 320 ± 10.13 that in Cd treated group, about 151 ± 16.50, while that in GSP-pretreated Cd intoxicated rats declined about 308 ± 14.72, to near the normal value.

3.12. Mitochondrial oxygen consumption

Respiratory activity of freshly isolated liver mitochondria from control and experimental rats, measured in the presence of pyruvate and malate, which drive the respiratory flux through complex I, and ADP to stimulate respiration, is reported in Fig. 10. Com-

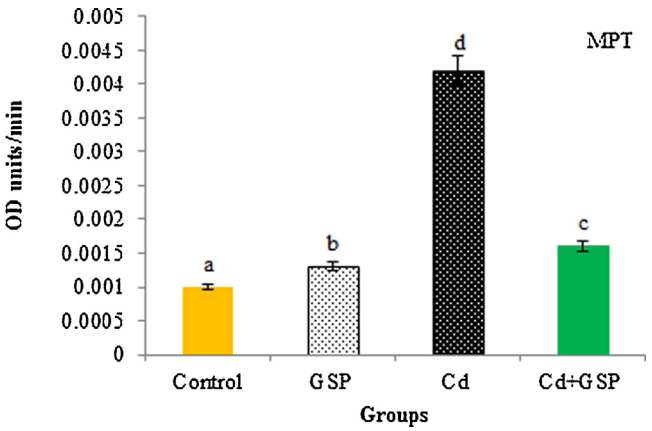

Fig. 8. Effects of GSP treatment on Cd-induced changes in mitochondrial permeability transition (MPT). Values are mean ± S.D. for six rats in each group. Bars not sharing a common superscript letter (a–d) differ significantly at $p < 0.05$ (DMRT).

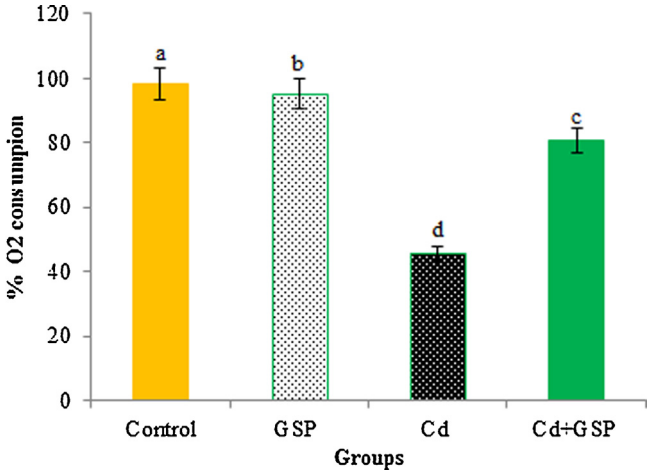

Fig. 10. Effects of GSP treatment on Cd-induced changes on complex I mediated oxygen consumption. Values are mean ± S.D. for six rats in each group. Bars not sharing a common superscript letter (a–d) differ significantly at $p < 0.05$ (DMRT).

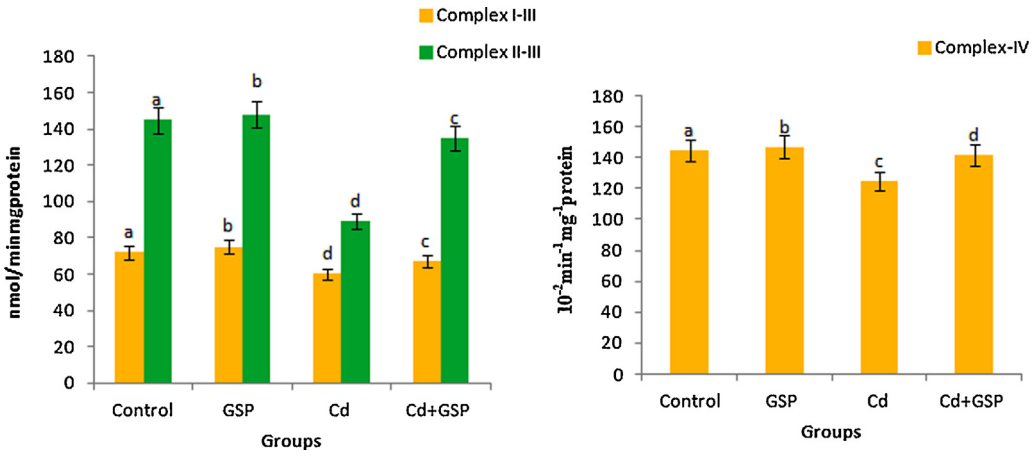

Fig. 11. Effects of GSP treatment on Cd-induced changes on complex I–III, complex IV and complex II–III in mitochondria of control and experimental rats. Values are mean ± S.D. for six rats in each group. Bars not sharing a common superscript letter (a–d) differ significantly at $p < 0.05$ (DMRT).

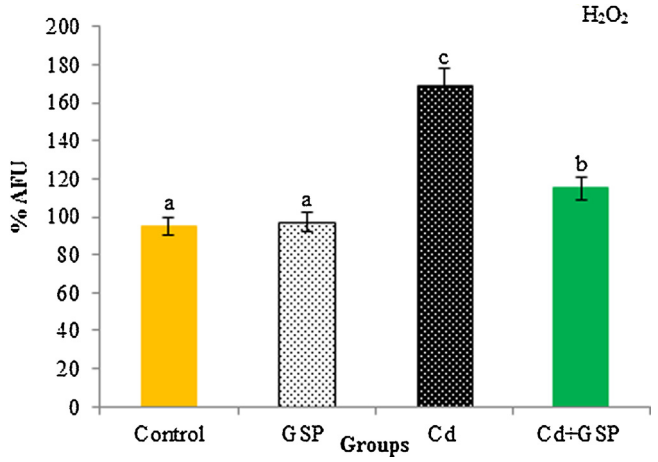

Fig. 12. Effect of GSP treatment on Cd induced H2O2 production in liver mitochondria of control and experimental rats. Values are mean ± S.D. for six rats in each group. Bars not sharing a common superscript letter (a–d) differ significantly at $p < 0.05$ (DMRT).

plex I substrate-mediated respiration was found to be significantly ($p < 0.05$) inhibited in Cd treated rats when compared to control rats. Pre-treatment of GSP to Cd intoxicated rats was found to be significantly ($p < 0.05$) restored the respiratory rate as compared to the Cd alone treated group.

3.13. Respiratory complexes activity

To further analyze the mitochondrial function, respiratory complexes activities were measured. Complex I–III, II–III and IV activity is shown in Fig. 11. The activity of complex I–III and complex IV was found to be significantly ($P < 0.05$) decreased in Cd treated rats as compared with control groups. The activities of Complex II–III were more inhibited on exposure to Cd as compared to the control rats. These decreased values returned to the corresponding control values significantly ($p < 0.05$) when Cd treated rats were pre-administrated with GSP as compared to the Cd alone treated rats.

3.14. Mitochondrial H_2O_2 production

The complex I mediated H_2O_2 generation significantly increased in liver mitochondria of the rats treated with Cd (Fig. 12). However, the pre-treatment of GSP to Cd treated rats significantly ($p < 0.05$) decreased H_2O_2 generation at complex I, when compared to Cd treated rats.

3.15. Effect of GSP on apoptotic signaling proteins

Fig. 13(A and B), shows the western blot analysis of signaling proteins in the liver of rats. The expression level of Caspase 3, Caspase 9, cytochrome c and FRAP significantly ($P < 0.05$) increased in the Cd-treated rats when compared to the control rats. To further confirm our findings, we have also measured the expression level of antiapoptotic proteins Bcl-2 and Bcl-*xL* and proapoptotic protein Bax. The level of Bax protein expression significantly ($P < 0.05$) increased with a significant ($P < 0.05$) decrease in the expression level of Bcl-2 and Bcl-*xL* protein in the liver tissues of Cd-treated rats when compared with control rats. Pretreatment of GSP (Fig. 4) in Cd intoxicated rats showed a significant ($P < 0.05$) decrease in the liver tissue levels of caspase-9, caspase-3, cytochrome c and PARP in the liver tissue as compared with Cd alone treated rats. Pretreatment of GSP in Cd treatment rats also showed a significant ($P < 0.05$) decrease in the level of Bax with significant ($P < 0.05$) increase in the level of Bcl-2 and Bcl-*xL* (Fig. 5) in the liver tissue when compared with Cd-treated rats. The group treated with GSP alone did not show any change in the levels of these apoptotic markers when compared with the control rats.

3.16. Electron microscopy

Fig. 14, reveals the electron microscopic examination of the control and experimental rat livers. The hepatocytes of control group have normal structures with well-distributed cytoplasm. The nucleus was normal with other organelles (Fig. 14A). In Cd-treated group, hepatocytes showed altered nucleus and degenerated mitochondria. Also, flattened nuclei, flattened microvilli with unevenly distributed glycogen and a number of lipid droplets were observed (Fig. 14C). Cd and GSP pretreated group revealed that the nucleus appeared normal with free ribosome and regular-shaped nuclei. Binucleated hepatocytes were abundant and evenly distributed heterochromatin and euchromatin were also seen (Fig. 14D). In GSP alone-treated group hepatocytes with normal mitochondria, rough endoplasmic reticulum was observed (Fig. 14B).

3.17. Effect of GSP on liver mitochondria ultra structure

The electron microscopic structure of the mitochondrial from the liver of control rats showed the normal liver mitochondria with a folded internal membrane, cristae-rich and a dense matrix, and

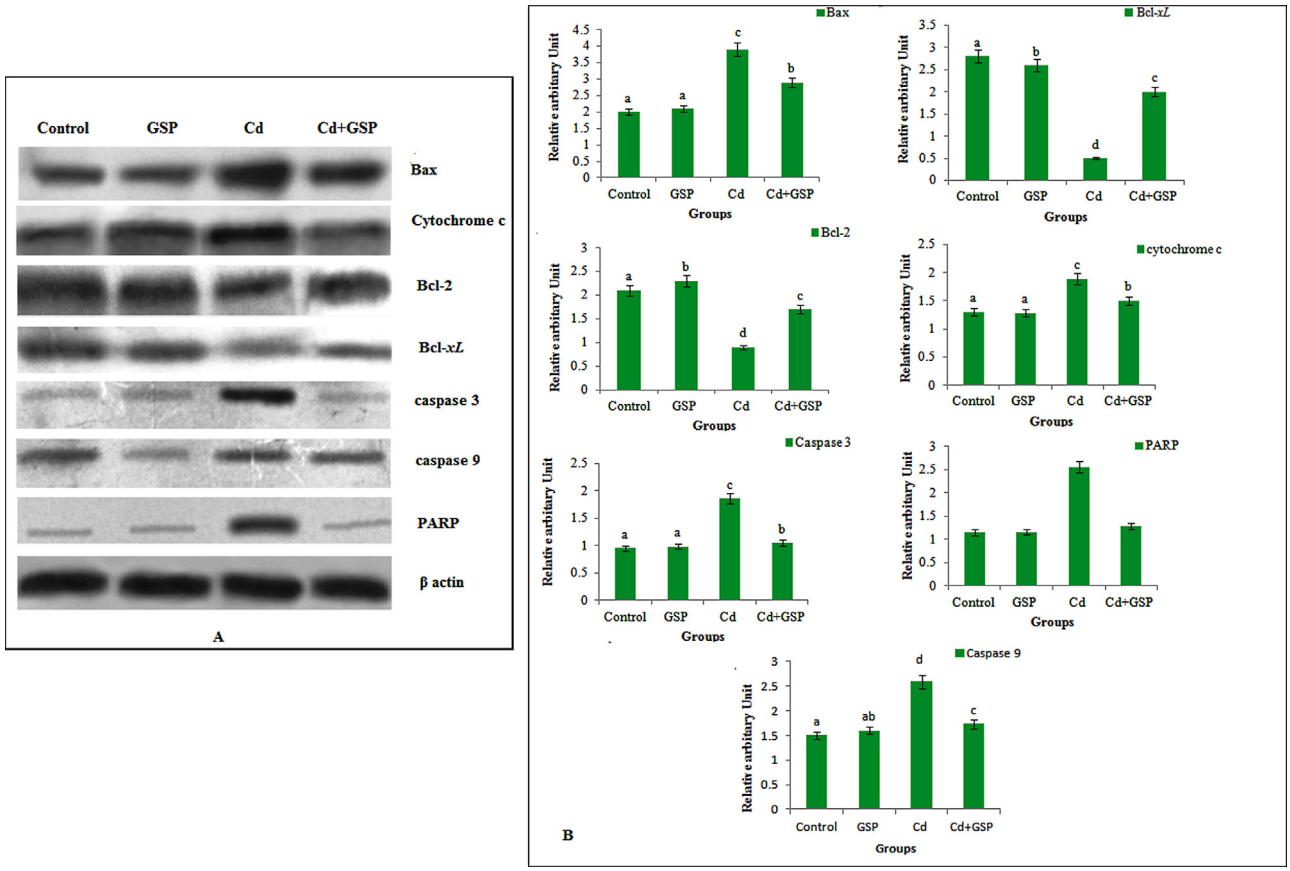

Fig. 13. Effect of GSP on western blot analysis of Bax, Bcl-2, Bcl-*xL*, cytochrome c, caspase 3, caspase 9 and PARP in liver tissue of control and experimental rats. Values are mean ± SD for groups of six rats in each. Values are given as mean ± S.D from six rats in each group. Bars with different superscript letter (a–d) differ significantly at $p < 0.05$ (DMRT).

was normal in volume (Fig. 15A). Liver mitochondria isolated from the rat treated with Cd showed a swollen mitochondria and disrupted cristae with vacuolation, destructurization of the matrix compartment and lack of dense granules (Fig 15C). Pre-treatment of GSP to Cd intoxicated rats showed mild swollen and vacuolated liver mitochondria with meek separated cristae when compared with Cd alone treated rats (Fig. 15D). In GSP alone treated rats the liver mitochondria showed a well preserved and normal architecture of the liver mitochondria (Fig. 15B).

4. Discussion

Cd is a widespread environmental and industrial pollutant prevailed in all parts and parcel of our environment. Humans and animals are exposed to Cd through a variety of means, including industrial contaminations, food sources especially sea foods and tobacco smoke. Cd, take part in an imperative role in inducing hepatocellular toxicity since the liver contributes to the rapid clearance of Cd from blood. Long term accumulation of Cd in the liver induced a variety of toxic responses in hepatocytes including production of ROS and oxidative damage. Cd has a long half- life period and resides in the body for about 15–30 years [1]. Due to its protracted half life in rats, Cd could continuously release into the body for a longer period of time. This prolonged exposure due to internal release could lead to oxidative stress and subsequent dysfunction of mitochondria, Fig. 16 .

In the present study, Cd induced oxidative stress seem to be correlated with the evidence of increased Cd content associated with biochemical changes in the liver. A different bio-kinetic pattern of Cd distribution facilitates its accumulation in the liver and causes oxidative stress. The liver is a highly perfused organ and provides a seat of all enzymatic reactions, including the production of metal binding proteins like metallothioneins (MT). Typically, the presence of MT within the hepatic cells markedly decreases upon Cd toxicity, because liver is the major site to detoxify the harmful effects of Cd by forming Cd-metallothionein complex and thus the choice of body's Cd accumulation site befalls liver. Unbound Cd reaches other organs where the active free metal ions again bind to membrane bound-SH containing groups [36]. Our results are in line with the findings of Elina et al. [37] which confirmed the higher accumulation of Cd in liver. GSP on the other hand protects against Cd induced accumulation and oxidative stress not only by its antioxidant property, but also by the metal chelating property which partially chelates the Cd ion and rendering it inactive.

The determination of membrane associated enzyme activities like adenosine triphosphatases (ATPases) indicates the changes in membrane under oxidative stress conditions [38]. In the present study, Cd significantly decreased the activities of membrane bound total ATPases in the liver and liver mitochondria in rats. Increased lipid peroxidation by ROS upon Cd intoxication decreases the activity of Na^+/K^+-ATPase, since Na^+/K^+-ATPase is a 'SH' group containing enzyme and is lipid dependent. It is generally accepted that due to the high affinity for SH groups, Cd binds avidly to various sulphydryl rich enzyme proteins and inactivates them. Decreased activity of Na^+/K^+-ATPase can lead to a decrease in sodium efflux, thereby altering the membrane permeability. The disruption of membrane permeability leads to the leakage of Ca^{2+} ions into cells, results in a higher concentration of Ca^{2+} in the liver mitochondria of rats, which decreases the Ca^{2+}-ATPase activity in the cell membrane, thereby potentiating irreversible cell destruction.

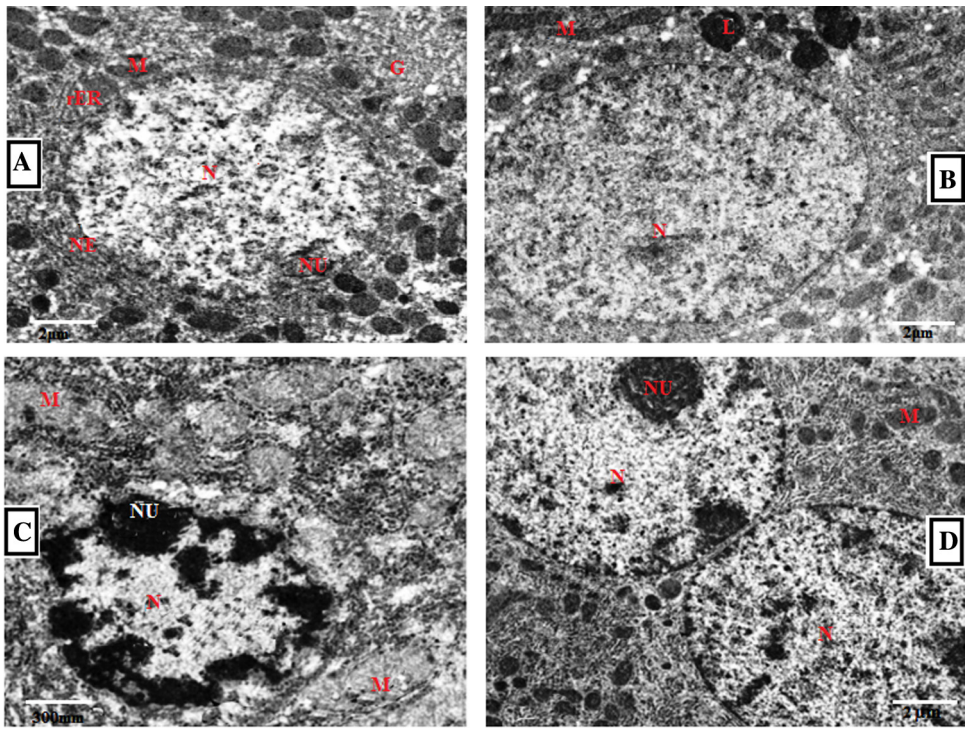

Fig. 14. Electron micrographs of liver in control and experimental rats. (A) Control group showing nucleus (N), nucleolus (NU), nuclear envelop (NE), Golgi (G), mitochondria (M) and rough endoplasmic reticulum (rER) with few fat droplets and well-distributed cytoplasm. The nucleus was normal with other organelles (B) GSP alone-treated group shows hepatocytes with normal mitochondria, rough endoplasmic reticulum, nucleus with few chromatin and lysosomes. Hepatocytes with large nucleus, evenly distributed chromatin were also seen. (C) Cd treated group showing pyknotic nucleus with abnormal envelop, degenerated mitochondria, flattened microvilli with unevenly distributed glycogen and a number of lipid droplets were observed (D) Cd and GSP-pretreated group showing Binucleated cell with normal nucleus, mitochondria, rough endoplasmic reticulum with dense chromatin. (5000×).

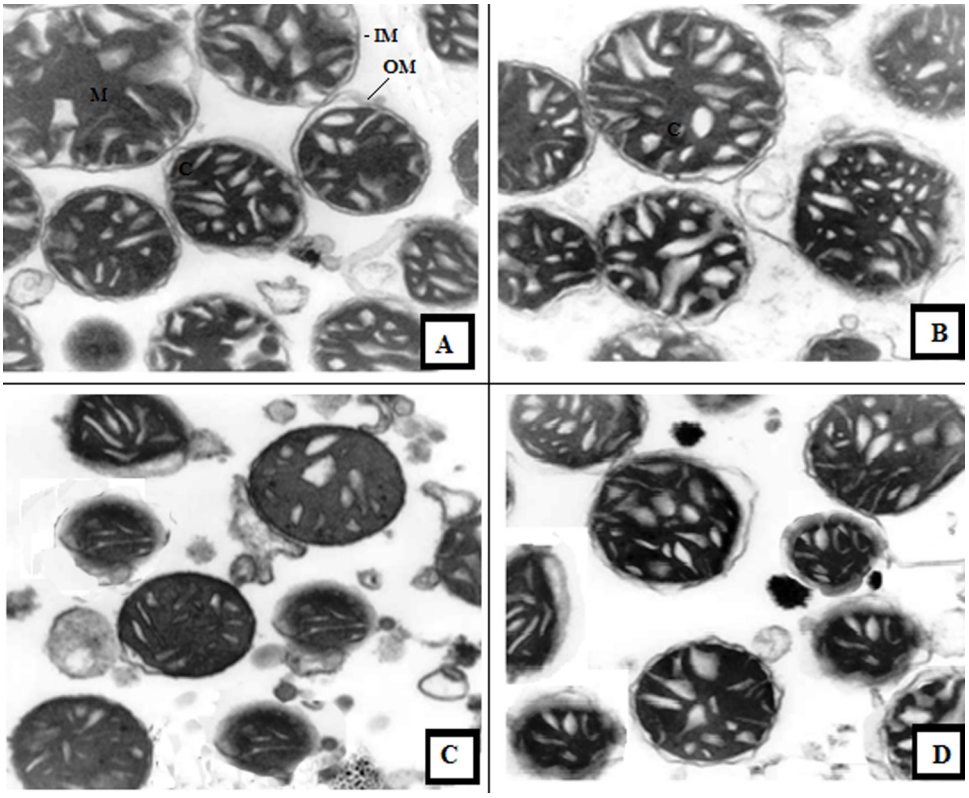

Fig. 15. Ultra structural study of liver mitochondria in control and experimental rats. (A) Mitochondria of control rats showed normal structural design with cristae (C), inner membrane (IM), outer membrane (OM) and it is well preserved. (B) In GSP alone treated rats the liver mitochondria shows well preserved and normal architecture. (C) Mitochondria isolated from the liver of rat treated with Cd shows swollen mitochondria and disrupted cristae with vacuolation. (D) Pre-treatment of GSP to Cd intoxicated rats show mild swollen and vacuolated liver mitochondria with mild separated cristae when compared with Cd alone treated rats. (15000×).

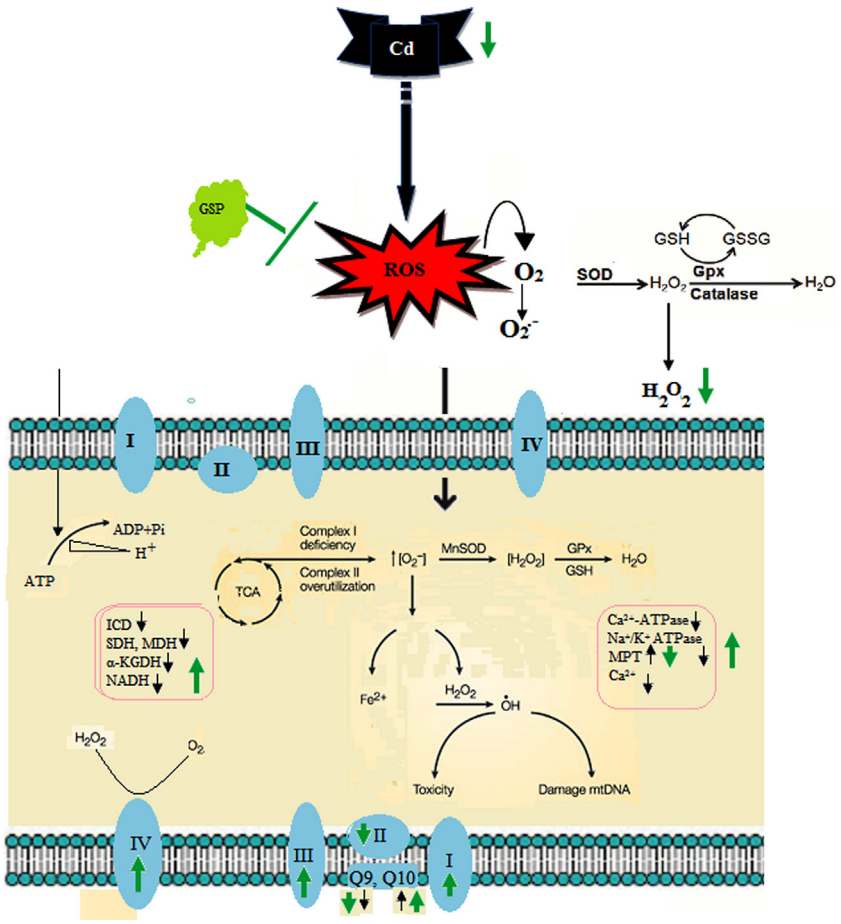

Fig. 16. Schematic diagram; black arrow: cadmium, green arrow: GSP.

Mg^{2+}-ATPase activity is involved in other energy requiring processes in the cell and its activity is sensitive to lipid peroxidation. Administration of GSP in Cd intoxicated rats significantly reduced the lipid peroxidation in the liver and in hepatic mitochondria and sustained the activities of membrane bound enzymes. This could be due to the ability of GSP to protect the activities of membrane bound ATPases because of its protection of -SH groups against oxidative stress via the free radical quenching action of di-OH (catechol) structure, present in the B ring of GSP [39]. Also the membrane stabilizing property, due to the blocking of lipid peroxidation in cell membranes by GSP abolishes the Cd-stimulated elevation of intracellular free Ca^{2+}concentration and restores the Cd-induced inhibition of Na^+, K^+, $Mg^{2+}$and Ca^{2+} -ATPases activities, which may be concerned with the protective effect of GSP on mitochondrial function and its efficacy in scavenging intracellular ROS [40].

Cd intoxication significantly elevated the levels of pro inflammatory cytokines TNF-α, IL-4 and NO in serum and increased the expression of hepatic NF-κB clearly suggesting Cd induced hepatic inflammation. The activation of NF-κB plays an important role in inflammation and cell proliferation. Increased ROS generation by free Cd ions in the liver through non Fenton reaction activates the NF-κB and is subsequently translocated into the nucleus where it regulates the transcription of response genes encoding inflammation associated enzymes such as IL-4 and TNF-α [41]. However, its activation and translocation to the nucleus was effectively inhibited by GSP. Activation of NF-κB is also achieved through the action of a family of serine/threonine kinases known as IKK. The IKK (IKKα and/or IKKβ) phosphorylate IκB proteins and the members of the NF-κB family. Therefore, the inhibitors of IKK have been considered as specific regulators of NF-κB activation. This can be attributed to up-regulation of inducible nitric oxide synthase (iNOS) by TNF-α increasing NO production [42]. NO reacts with the superoxide anion to produce peroxynitrite radical inducing further cell damage, by the depletion of intracellular GSH and increasing the vulnerability to oxidative stress. On the other hand, preadministration of GSP effectively suppresses inflammation through the inhibition of NF-κB signal transduction pathways. Our study suggests that the inhibitory effect of GSPs on Cd-induced NF-κB activation may be mediated through the inhibition of proteolysis of the IκBα protein.

It is well documented that IκBα binds to NF-κB through a protein–protein interaction, and thus this interaction prevents migration of NF-κB into the nucleus [43]. Further GSP suppresses IκK activation, and the inactivated IκK complex suppresses the phosphorylation-induced degradation of IκBα. Therefore the NF-κB activation signal can be abrogated by newly-synthesized IκBα, which enters the nucleus, removes NF-κB dimers from DNA, and results in their export in mediated transport to the cytoplasm [44]. In concordance, we reported a dramatic increase in Hyp and TGF-β1contents in the liver of Cd-treated rats, suggesting the signs of fibrosis in Cd treated rats. GSP pretreatment blocked the Cd-induced collagen production as evidenced by the reduced Hydroxyproline and TGF-β1 contents in the liver of rats. This might be possibly attributed to the ROS scavenging action of GSP polyphenols especially the tannins present in it.

In our study, we found a significant decline in the activities of mitochondrial ICDH, SDH, MDH, α-KDH and NADH dehydrogenase in Cd-intoxicated rats. Cd induced oxidative stress reduces the activities of tri-carboxylic acid cycle enzymes (TCA), which could disturb the mitochondrial phospholipid bilayer, lead to an increase in the levels of lipid peroxidation via altering the electron transport

or respiratory chain complex [45] and thereby decreased the activities of these mitochondrial enzymes. Pre administration of GSP in Cd treated rats caused a significant elevation in the activities of the TCA cycle enzymes. GSP produced a significant uncoupling in mitochondria isolated from the liver of rats using both pyruvate and carnitine palmitoyl-CoA as substrates. A slight uncoupling of oxidative phosphorylation in liver is related to a protective effect against oxidative stress and decreased production of ROS, which is one of the reasons for improved mitochondrial function as well as hepatic protection of GSP in Cd-intoxicated rats.

In the present study, we observed a significant inhibitory effect of Cd on mitochondrial membrane potential (MPT) and Membrane Permeability Transition ($\Delta\Psi m$) which could reflect the integrity and function of mitochondria in Cd treated rats. Cd directly lead to the dysfunction of mitochondria, including the inhibition of respiration, the opening of PTP, the loss of membrane potential and the release of cytochrome c. The PTP is a protein-complex, which lies in the contact site between inner and outer membrane of mitochondria. PTP is thought to contain hexokinase, voltage-dependent anion channel (VDAC), creatine kinase, the adenine nucleotide translocator (ANT) and cyclophilin D (CyP-D) [46]. Our research has revealed that Cd probably acted on ANT to trigger the opening of PTP. Cd entered mitochondria via Ca^{2+} uniporter and only took an effect inside mitochondria. ANT lied in the inner membrane and was easily attacked by Cd. This results in a rapid ion movement followed by extensive mitochondrial swelling and loss of the mitochondrial membrane potential [47]. On the other hand, GSP pretreatment shows decreased/controlled MPT function by rescuing the levels of these proteins and brought back the expression to near normal levels in Cd treated rats. Our findings support the possibility that changes in these proteins during GSP pretreatment, directly or indirectly act on ANT and inhibit the pore opening. This implies the restoration capacity and membrane-stabilizing potential of GSP on hepatic mitochondria.

Ubiquinones (co-enzymes Q9 and Q10) function as important cellular electron carriers, distributed in the intracellular major organelles principally in mitochondria. In our study, the coenzyme Q9 and Q10 were significantly decreased in the tissues of Cd intoxicated rats. These changes might be attributed to the increased level of Cd that may disrupt the activity of the enzymes responsible for the reduction of ubiquinone to ubiquinol [48]. GSP exerts its protective effect on ubiquinones levels through promoting the clearance of Cd from the liver mitochondria through its metal chelating action. Moreover, GSP is a good vehicle for the enrichment of Q10 and Q9 in the body because of its remarkable antioxidant capacity.

The respiratory complex is considered as an important site of superoxide anion generation in mitochondria [5] and thus a potential source of ROS in the liver. In our study, we observed a significant inhibition for mitochondrial complex I–III and complex IV in the liver mitochondria of Cd treated rats but the Complex II and III, showed maximum inhibition in Cd treated rats. Our findings are in concurrent with the other published reports, which stated that the activities of complexes II and III were more inhibited on exposure to Cd [45]. In our findings, the impairment of electron transfer through complex II and III by Cd, might possibly be the major route of ROS generation as Cd can bind to complex III resulting in the accumulation of unstable semiubiquinones, which then transfer an electron to molecular oxygen, resulting in the formation of superoxide ions [45]. Another possibility to be considered is interference of Cd with Iron-S (Fe-S) centers of complex I in the liver of Cd intoxicated rats, which might be the results in the inhibition of complex I and III [45]. The exact molecular mechanism of GSP and respiratory complex enzymes is not known. But in our present study, GSP supplementation improves the mitochondrial function (with pyruvate as substrate) and produced an increase of all inhibited complexes in the liver mitochondria of rats. GSP produced a significant uncoupling in mitochondria isolated from the liver of rats, a slight uncoupling of oxidative phosphorylation in liver is related to a protective effect against oxidative stress and decreased production of ROS in mitochondria [49].

Complex I, also considered, being an important site of mitochondrial oxygen radical production. It is reasonable to assume that the impairment of complex I, observed in the mitochondria from Cd treated liver, attributed to the ROS induced damage and increased the electron leak from the electron transport chain, through cytochrome c, generating more superoxide radicals and perpetuating a cycle of oxygen radical-induced mitochondrial membrane damage which ultimately leads to hepatocyte injury [50]. Also the variations in the cytochrome c content observed in Cd treated rats affects the transport of electrons through the electron transport chain and thereby altering the energy production. Cd increased lipid peroxidation has been reported to alter the lipid environment of the membrane, thus affecting the activity of some respiratory chain enzymes like cytochrome c oxidase [51]. A decrease in liver mitochondrial cytochrome c content could result in a concomitant loss of oxidative phosphorylation [52]. Pretreatment with GSP significantly attenuated the alterations in the activity of mitochondrial cytochrome c, thereby restoring the mitochondrial function. The flavonoids present in GSP, with their high antioxidant property, might have been responsible for the maintenance of the electron transport chain by scavenging the free radicals. Moreover, the high level of mitochondrial respiration induced by the pretreatment with GSP in mitochondrial respiratory states, provide the information that the mitochondrial capacity to oxidize NADH and FADH2 from the citric acid cycle or β-oxidation in the ETC, resulting in the oxidative phosphorylation of ADP to ATP by ATPase and thereby restores the mitochondrial respiration which was altered by Cd [53].

Mitochondria participates a vital role in regulating apoptosis. To confirm the protection of GSP in Cd induced apoptosis in the liver of rats, we performed immunoblot analyses of Bax, Bcl-2, Bcl-*xL* and caspase 3, caspase 9, cytochrome c and PARP in our study. It was observed that Cd intoxication up-regulated (pro-apoptotic) Bax and down-regulated (anti-apoptotic) Bcl-2 and Bcl-*xL* proteins and increased the concentration of effector caspase 3, initiator caspase 9, cytochrome c and PARP in the liver of rats. Cd mediated apoptosis occurs primarily through two well-recognized pathways intrinsic or mitochondrial-mediated pathway, and the extrinsic or death receptor-mediated pathway [54,40]. Kondah et al. [55] has reported that Cd induces the activation of caspase 9 prior to DNA fragmentation. Caspase 3 is a caspase downstream of caspase 9. Therefore, it is suggested that Cd induced apoptosis is partly dependent on the mitochondrial pathway which is accompanied by caspase activation. Whereas, Cd increased cytochrome c in the liver of rats and disrupts the Bcl-2 family protein, reduces the expression of Bcl-2, Bcl-*xL* and increases the expression of Bax. Our immunoblotting studies have confirmed that GSP caused a decrease in the levels of Bax, caspase 9 by decreasing the level of free radicals, consequently maintaining the mitochondrial membrane permeability. The anti-apoptotic effect of GSP works by means of increasing the expression of Bcl-*xL*, a member of the bcl-2 family that establishes the resistance to apoptotic cell death [56]. The level of caspase-3 gradually decreased after GSP treatment, indicating that falls of caspase-3 restores the mitochondrial enzyme pathway. The evidence for caspase-3 deactivation is proved in our study by the subsequent decrease in cleavage of the caspase-3 substrate PARP in GSP-pretreated Cd intoxicated rats [40].

The comet assay is a hasty, perceptive and resourceful method for the quantification of DNA damage in individual cells. In the present study, the level of % DNA in tail, tail length and tail movement was significantly increased in the hepatocytes of Cd treated

rats. Earlier reports showed that ROS and enhanced lipid peroxidation are involved in DNA damage induced by Cd [57]. According to Whiteman et al. [58] semiubiquinones present in mitochondria are prone to transfer one electron to molecular oxygen to form superoxide ions, providing a potential mechanism for Cd-induced generation of ROS, which results in DNA damages, such as DNA strand breaks and base modifications. Preadministration of GSP in Cd treated rats' protected DNA fragmentation in the liver of rats due to its free radical scavenging and antiendonucleolytic activity. Moreover, proanthocyanidins protects DNA damage due to the detoxification of cytotoxic radicals and their reactive metabolites through its extensive free radical scavenging and antioxidant efficacy and thereby reduces the DNA damage [59].

In the present study, Cd induced liver mitochondrial injury is confirmed by the ultra structural changes. Cd induced many alternations in liver ultra structure and liver mitochondria. Nuclear membrane rupture and lysosomes were observed in the liver cytoplasm, rupture of mitochondrial cristae and glycogen granules were observed in the liver of Cd treated rats. Cd also caused a fragmentation in rough endoplasmic reticulum and swollen mitochondria [60]. The vaculation of the liver cells can be attributed to swelling of the mitochondria and proliferation of the endoplasmic reticulum in liver of Cd treated rats. However, preadministration of GSP markedly reduced the histological alterations provoked by Cd and restored its ultra structure. This can be attributed to the antioxidant and free radical quenching efficacy of GSP. Also, the unique polyhydroxy phenolic groups of proanthocyanidins exert an enhanced antioxidant effect which significantly reduced the oxidative stress elicited by Cd.

To summarize, it may be interpreted that our study has proved another characteristic and appropriate mechanism of GSP protection against Cd induced hepatotoxicity in rats at the mitochondria level. Our results showed that GSP significantly rescued the Cd induced hepatic DNA damage, apoptosis, inflammation and ultra structural alterations and counteracted the Cd induced biochemical and structural alterations in liver mitochondria owing to its free radical scavenging, antioxidant and metal chelating properties. These findings strengthened the mitoprotective nature of GSP. Further in-depth studies are warranted to delineate the molecular mechanisms of Cd induced mitochondrial toxicity and the structure activity based protective effects of GSP on rat liver mitochondria.

Transparency document

The Transparency document associated with this article can be found in the online version.

Acknowledgements

The Authors would like to thank Professor and Head of the Department of Zoology, Annamalai University and UGC-MANF (MANF-2013-14-MUS-JAM-23333) New Delhi for providing the fellowship to one of the author Nazimabashir is greatly acknowledged.

References

[1] S.J. Stohs, D. Bagchi, E. Hassoun, M. Bagchi, Oxidative mechanisms in the toxicity of chromium and cadmium ions, J. Environ. Pathol. Toxicol. Oncol. 20 (2001) 77–88.
[2] L.E. Rikans, T. Yamano, Mechanisms of cadmium-mediated acute hepatotoxicity, Biochem. Mol. Toxicol. 14 (2000) 110–117.
[3] R.E. Dudley, D.J. Svoboda, C.D. Klaassen, Time course of cadmium-induced ultrastructural changes in rat liver, Toxicol. Appl. Pharmacol. 76 (1984) 150–160.
[4] F. Kayama, T. Yoshida, M.R. Elwell, M.I. Luster, Role of tumor necrosis factor-alpha in cadmium-induced hepatotoxicity, Toxicol. Appl. Pharmacol. 131 (1995) 224–234.
[5] A. Boveris, B. Chance, The mitochondrial generation of hydrogen peroxide: general properties and effect of hyperbaric oxygen, Biochem. J. 134 (1973) 707–716.
[6] W. Tang, Z.A. Shaikh, Renal cortical mitochondrial dysfunction upon cadmium metallothionein administration to Sprague-Dawley rats, J. Toxicol. Environ. Health. A 63 (2001) 221–235.
[7] D. Bagchi, M. Bagchi, S.J. Stohs, S.D. Ray, C.K. Sen, H.G. Pruess, Cellular protection with proanthocyanidins derived from grape seeds, Ann. N. Y. Acad. Sci. 957 (2002) 260–270.
[8] I. Spranger, B. Sun, A.M. Mateus, V. Freitas, J.M. Ricardo-da-Silva, Chemical characterization and antioxidant activities of oligomeric and polymeric procyanidin fractions from grape seeds, Food Chem. 108 (2008) 519–532.
[9] D. Bagchi, A. Garg, R. Krohn, et al., Protective effects of grape seed proanthocyanidins and selected antioxidants against TPA-induced hepatic and brain lipid peroxidation and DNA fragmentation, and peritoneal macrophage activation in mice, Gen. Pharmacol. 30 (1998) 771–776.
[10] Nazimabashir, V. Manoharan, S. Milton Prabu, Protective role of grape seed proanthocyanidins against cadmium induced hepatic dysfunction in rats, Toxicol. Res. 3 (2014) 131–141.
[11] M. Lagouge, C.Z. Argmann Gerhart-Hines, H. Meziane, C. Lerin, F. Daussin, N. Messadeq, J. Milne, P. Lambert, B. Elliott, M. Geny, P. Laakso, J. Puigserver, Auwerx, Resveratrol improves mitochondrial function and protects against metabolic disease by activating SIRT1 and PGC-1 alpha, Cell 127 (2006) 1109–1122.
[12] D.C. Nieman, A.S. Williams, R.A. Shanely, F. Jin, S.R. McAnulty, N.T. Triplett, M.D. Austin, D.A. Henson, Quercetin's influence on exercise performance and muscle mitochondrial biogenesis, Med. Sci. Sports Exerc. 42 (2010) 338–345.
[13] J. Renugadevi, S.M. Prabu, Cadmium-induced hepatotoxicity in rats and the protective effect of naringenin, Exp. Toxicol. Pathol. 62 (2010) 171–181.
[14] H. Evans, J. Giglio, Interferences in inductively coupled plasma mass spectrometry, J. Anal. At. Absorpt. Spectrom. 8 (1993) 1–18.
[15] S.L. Bonting, Membrane and Ion Transport, Presence of Enzyme Systems in Mammalian Tissues, Wiley Interscience, London, 1970, pp. 257–263.
[16] T. Ohnishi, T. Suzuki, Y. Suzuki, et al., A comparative study of plasma membrane Mg^{2+}-ATPase activities in normal, regenerating and malignant cells, Biochim. Biophys. Acta Biomembr. 684 (1982) 67–74.
[17] O.H. Lowry, N.J. Rosebrough, A.L. Farr, et al., Protein measurement with the folin phenol reagent, Biol. Chem. 193 (1951) 265–275.
[18] D.R. New, S.B. Maggirwar, L.G. Epstein, S. Dewhurst, H.A. Gelbard, HIV-1 rat induces neuronal death via tumor necrosis factor-alpha and activation of non-*N*-methyl-D-aspartate receptors by a NF-kB-independent mechanism, J. Biol. Chem. 273 (1998) 17852–17858.
[19] D. Javelaud, A. Mauviel, Mammalian transforming growth factor betas: smad signaling and physio-pathological roles, Int. J. Biochem. Cell Biol. 36 (2004) 1161–1165.
[20] Y. Nolan, F.O. Maher, D.S. Martin, R.M. Clarke, M.T. Brady, A.E. Bolton, et al., Role of interleukin-4 in regulation of age-related inflammatory changes in the hippocampus, J. Biol. Chem. 280 (2005) 9354–9362.
[21] M. Fujita, J.M. Shannon, O. Morikawa, J. Gauldie, N. Hara, R.J. Mason, Overexpression of tumor necrosis factor-α diminishes pulmonary fibrosis induced by bleomycin or transforming growth factor-β, Am. J. Respir. Cell Mol. Biol. 29 (2003) 669–676.
[22] N.P. Singh, Microgels for estimation of DNA strand breaks, DNA protein crosslinks and apoptosis, Mutat. Res. 455 (2000) 111–127.
[23] K. Cain, D.N. Skilleter, Preparation and use of mitochondria in toxicological research, in: K. Snell, B. Mullock (Eds.), Biochemical Toxicology—A Practical Approach, IRL, Press, England, Oxford, 1987, pp. 221–223.
[24] S. Fleischer, G. Rouser, B. Fleisher, A. Casu, Kritchevsky lipid composition of mitochondria from bovine heart liver and kidney, J. Lipid Res. 8 (1967) 170–179.
[25] J. King, Isocitrate dehydrogenase, in: J.C. King, D. Van (Eds.), Practical Clinical Enzymology, Van Nostrand Co Ltd, London, 1965, pp. 257–363.
[26] L.J. Reed, R.B. Mukherjee, α-Ketoglutarate dehydrogenase complex from *E. coli*, in: J.M. Lowenstein (Ed.), Methods in Enzymology, Academic Press, London, 1969, pp. 53–61.
[27] S. Minakami, R.L. Ringer, T.P. Singer, Studies on the respiratory chain linked dehydro diphosphopyridine nucleotide dehydrogenase I. Assay of the enzyme in particulate and in soluble preparation, J. Biol. Chem. 237 (1962) 569–576.
[28] Y. Zhang, F. Aberg, E.L. Appelkvist, G. Dallner, L. Ernster, Uptake of dietary coenzyme Q supplement is limited in rats, J. Nutr. 125 (1995) 446–453.
[29] G. Rorive, A. Kleinzellar, Ca^{2+} activated ATPase from renal tubular cells, Methods. Enzymol. 32 (1974) 303–306.
[30] O.H. Lowry, J.A. Lopez, The determination of inorganic phosphate in the presence of labile phosphate esters, J. Biol. Chem. 162 (1946) 421–428.
[31] M.M. Zydowo, J. Swiercynski, G. Nagel, T. Wrzolkowo, The respiration and calcium content of heart mitochondria from rats with vitamin D-induced cardio necrosis, J.Biochem. 226 (1985) 155–161.
[32] P.X. Petit, M. Goubern, P. Diolez, S.A. Susin, N. Zamzami, G. Kroemer, Disruption of the outer mitochondrial membrane as a result of large amplitude swelling: the impact of irreversible permeability transition, FEBS Lett. 426 (1998) 111–116.
[33] R.K. Emaus, R. Grunwald, J.J. Lemasters, Rhodamine 123 as a probe of transmembrane potential in isolated rat-liver mitochondria: spectral and metabolic properties, Biochim. Biophys. Acta. 85 (1986) 436–448.
[34] J.M. Graham, D. Rickwood, Subcellular fraction, 1st (ed.), in: A Practical Approach, Oxford University Press, USA, 1997, pp. 120–128.

[35] M.K. Paul, M. Patkari, A.K. Mukhopadhayay, Existence of a distinct concentration window governing daunorubicin induced mammalian liver mitotoxicity-implication for determining therapeutic window, Biochem. Pharmacol. 74 (2007) 821–830.
[36] N. Ercal, H. Gurer-Orhan, N. Aykin-Burns, Toxic metals and oxidative stress part I: mechanisms involved in metal-induced oxidative damage, Curr. Top. Med. Chem. 1 (2001) 529–539.
[37] M. Elina, K.G. Arnab, G. Debosree, B.F. Syed, M. Debasri, C. Aindrila, K.P. Sanjib, D. Santanu, B. Debasish, Ameliorative effect of aqueous curry leaf (*murraya koenigii*) extract against cadmium-induced oxidative stress in rat liver: involvement of antioxidant mechanisms, Int. J. Pharm. Sci. 2 (2013) 570–583.
[38] R.K. Kempaiah, K. Srinivasan, Protective effect of curcumin, capsaicin and garlic on erythrocyte integrity in high fat fed rats, J. Nutritional. Biochem. 17 (2006) 471–478.
[39] K. Ishige, D. Schubert, Y. Sagara, Flavonoids protect neuronal cells from oxidative stress by three distinct mechanisms, Free. Radic. Biol. Med. 30 (2001) 433–446.
[40] V. Nazimabashir, S.M. Manoharan, iltonprabu, Grape seed proanthocyanidins ameliorates cadmium-induced renal injury and oxidative stress in experimental rats through the up-regulation of nuclear related factor 2 and antioxidant responsive elements, Biochem. Cell Biol. 93 (2015) 1–17.
[41] S. Bhaskar, V. Shalini, A. Helen, Quercetin regulate oxidized LDL induced inflammatory changes in human PBMCs by modulating the TLR NF-κB signaling pathway, Immunobiology 216 (2011) 367–373.
[42] S.M. Morris Jr., T.R. Billiar, New insights into the regulation of inducible nitric oxidesynthesis, Am. J. Physiol. 266 (1994) 829–839.
[43] P.A. Baeuerle, D. Baltimore, NF-kB: ten years after, Cell 87 (1996) 13–20.
[44] X. Li, X. Yang, Y. Cai, H. Qin, L. Wang, Y. Wang, et al., Proanthocyanidins from grape seeds modulate the NF-kB signal transduction pathways in rats with TNBS-induced ulcerative colitis, Molecules 16 (2011) 6721–6731.
[45] Y. Wang, J. Fang, S.S. Leonard, K.M. Rao, Cadmium inhibits the electron transfer chain and induces reactive oxygen species, Free. Radic. Biol. Med. 36 (2004) 1434–1443.
[46] N. Zamzami, G. Kroemer, The mitochondrion in apoptosis: how pandora's box opens, Nat. Rev. 2 (2001) 67–71.
[47] K.S. Min, H. Kim, M. Fujii, N. Tetsuchikawahara, S. Onosaka, Glucocorticoids suppress the inflammation-mediated tolerance to acute toxicity of cadmium in mice, Toxicol. Appl. Pharmacol 178 (2002) 1–7.
[48] T. Kishi, T. Takahashi, A. Usui, T. Okamoto, Ubiquinone redox cycle as a cellular antioxidant defense system, Biofactors 10 (1999) 131–138.
[49] K.S. Echtay, J.L. Pakay, T.C. Esteves, M.D. Rand, Hydroxynonenal and uncoupling proteins: a model for protection against oxidative damage, Biofactors 24 (2005) 119–130.
[50] G. Petrosillo, P. Portincasa, I. Grattagliano, G. Casanova, M. Matera, M.R. Francesca, F. Domenico, P. Giuseppe, Mitochondrial dysfunction in rat with nonalcoholic fatty liver involvement of complex I, reactive oxygen species and cardiolipin, BBA (2007) 1260–1267.
[51] L. Trumper, B. Hoffman, T. Wiswedel, et al., Impairment of the respiratory chain in b-c1 region as early functional event during fe2+/ascorbate induced peroxidation in rat liver mitochondria, Biomed. Biochim. Acta. 47 (1988) 933–939.
[52] L.R. Bush, H. Shlafer, D.W. Haack, et al., Time dependent changes in canine cardiac mitochondrial function and ultra structure resulting from coronary occlusion and reperfusion, Basic. Res. Cardiol. 75 (1980) 553–571.
[53] E. Aguirre, S. Cadenas, GDP and carboxyatractylate inhibit 4-hydroxynonenal-activated proton conductance to differing degrees in mitochondria from skeletal muscle and heart, Biochim. Biophys. Acta. 1797 (2010) 1716–1726.
[54] T. Eichler, Q. Ma, C. Kelly, J. Mishra, S. Parikh, R.F. Ransom, P. Devarajan, W.E. Smoyer, Single and combination toxic metal exposures induce apoptosis in cultured murine podocytes exclusively via the extrinsic caspase 8 pathway, Toxicol. Sci. 90 (2006) 392–399.
[55] M. Kondah, S. Araragi, K. Sato, M. Higashimoto, M. Takiguchi, M. Sato, Cadmium induces apoptosis partly via caspase-9 activation in HL-60 cells, Toxicology 170 (2002) 111–117.
[56] S.D. Ray, M.A. Kumar, D.A. Bagchi, Novel proanthocyanidin IH636 grape seed extract increases *in vivo* Bcl-XL expression and prevents acetaminophen-induced programmed and unprogrammed cell death in mouse liver, Arch. Biochem. Biophys. 369 (1999) 42–58.
[57] A. Traore, S. Ruiz, I. Baudrimont, et al., Combined effects of okadaic acid and cadmium on lipid peroxidation and DNA bases modifications (m5dC and 8-(OH)-dG) in Caco-2 cells, Arch. Toxicol. 74 (2000) 79–84.
[58] M. Whiteman, H.S. Hong, A. Jenner, et al., oss of oxidized and chlorinated bases in DNA treated with reactive oxygen species: implications for assessment of oxidative damage in vivo, Biochem. Biophys. Res. Commun. 296 (2002) 883–889.
[59] S.D. Ray, D. Patel, V. Wong, D. Bagchi, In vivo protection of DNA damage associated apoptotic and necrotic cell deaths during acetaminophen-induced nephrotoxicity, amiodarone-induced lung toxicity and doxorubicin induced cardio toxicity by a novel IH636 grape seed proanthocyanidin extract, Res. Commun. Mol. Pathol. Pharmacol. 107 (2000) 137–166.
[60] W.M. Abdel-Moneim, H.H. Ghafeer, J. Mansoura, The potential protective effect of natural honey against cadmium induced hepatotoxicity and nephrotoxicity, Forensic Med. Clin. Toxicol. 15 (2007) 75–98.